Implementation of Damage Tolerance Concepts Into Stress-Based Fatigue Dimensioning Guidelines

H.-P. Gaenser[1, a], J. Froeschl[1,b] and W. Eichlseder[1,c]

[1]Chair of Mechanical Engineering, University of Leoben, A-8700 Leoben, Austria

[a]gaenser@mu-leoben.at, [b]juergen.froeschl@mu-leoben.at, [c]wilfried.eichlseder@mu-leoben.at

Keywords: stress concentration, flaw, notch, dimensioning, endurance limit, damage tolerant design, Haigh diagram

Abstract. Many real-life engineering components exhibit intrinsic flaws from manufacturing or operation. In this contribution, concepts from fracture mechanics are implemented into classical mechanical engineering approaches such as fatigue notch factors and Haigh diagrams in order to apply the latter methods to the dimensioning of components containing flaws.

Introduction

In the traditional design approach, unflawed components made of a homogeneous material are assumed; they are dimensioned against fatigue with respect to an allowable local maximum stress amplitude. However, real-life engineering materials usually exhibit intrinsic flaws such as precipitates or voids; and real-life engineering components very often are subject to some damage during manufacturing (such as forging defects or quenching cracks) or in operation (foreign object damage). Traditionally, such influences have been accounted for by means of empirical correction factors. However, from a physical point of view, they are best assessed by means of fracture mechanics. In this contribution, a connection is made between concepts from fracture mechanics and classical approaches such as Haigh diagrams (accounting for the mean stress influence) and fatigue notch factors (accounting for gradient and size effects) in order to apply the latter methods to the dimensioning of components containing flaws.

Mean Stress Influence – Haigh Diagram

Following El Haddad *et al.* [1], the dependence of the stress range $\Delta\sigma$ endurable at the fatigue limit on the size a of a surface defect is represented well by the empirical equation

$$\Delta\sigma = \frac{\Delta K_{\mathrm{th}}}{Y\sqrt{\pi(a+l_0)}}\,, \tag{1}$$

where ΔK_{th} is the threshold stress intensity factor (SIF) range for the propagation limit of mechanically long cracks, and the intrinsic length parameter l_0 is estimated by

$$l_0 = \frac{1}{\pi}\left(\frac{\Delta K_{\mathrm{th}}}{Y\,\Delta\sigma_{\mathrm{lim},0}}\right)^2 = \frac{1}{\pi}\left(\frac{\Delta K_{\mathrm{th}}}{2Y\,\sigma_{\mathrm{a0}}}\right)^2, \tag{2}$$

with σ_{a0} denoting the fatigue limit stress amplitude and $\Delta\sigma_{\mathrm{lim},0} = 2\sigma_{\mathrm{a0}}$ denoting the fatigue limit stress range of unflawed specimens. Y is a correction factor depending on the geometry, taking a value of 1.1215 for small surface flaws.

Inserting the expression for the length parameter, Eq. (2), into Eq. (1) gives

$$\sigma_a = \frac{\Delta\sigma}{2} = \frac{\Delta K_{th}}{2Y\sqrt{\pi(a+l_0)}} = \frac{\Delta K_{th}}{2Y\sqrt{\pi\left[a+\frac{1}{\pi}\left(\frac{\Delta K_{th}}{Y\Delta\sigma_{lim,0}}\right)^2\right]}}. \quad (3)$$

After algebraic simplification, the fatigue limit stress amplitude σ_a of a specimen containing a flaw of size a is given by

$$\sigma_a = \frac{1}{\sqrt{\frac{4\pi Y^2 a}{\Delta K_{th}{}^2} + \frac{1}{\sigma_{a0}{}^2}}}, \quad (4)$$

with the threshold SIF range ΔK_{th} and the fatigue limit stress amplitude of the unflawed material σ_{a0} themselves depending on the stress ratio R [2].

The dependence of the threshold stress intensity range on the stress ratio is well approximated by a bi-linear function (Fig. 1) [3]. The fatigue limit stress amplitude of the unflawed material may be read directly from the Haigh diagram of the unflawed material, see the filled circles in Fig. 2. With this data, Eq. (4) gives the fatigue limit stress amplitude of the material containing flaws of size a. (filled squares in the Haigh diagram, Fig. 2).

In such a flaw size dependent Haigh diagram, Fig. 2, it is clearly visualized that there exist four complementary limits for the fatigue strength of a flawed component:

- the Goodman line of the unflawed material,
- the yield limit of the unflawed material,
- the stress intensity amplitude threshold for fatigue crack growth (ΔK limit),
- the maximum stress intensity threshold for fatigue crack growth (K_{max} limit).

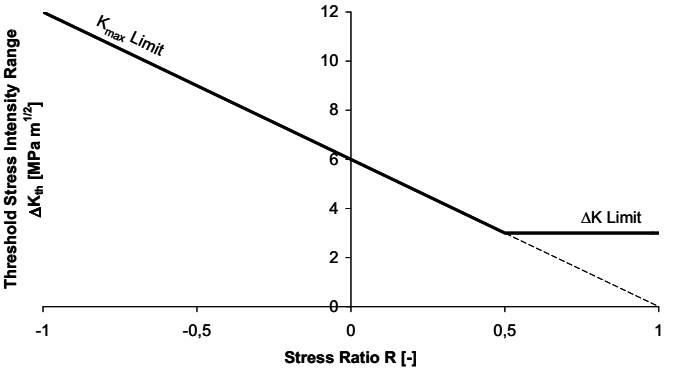

Fig. 1: Dependence of the threshold SIF range on the stress ratio; typical values for QT steels, after [3]

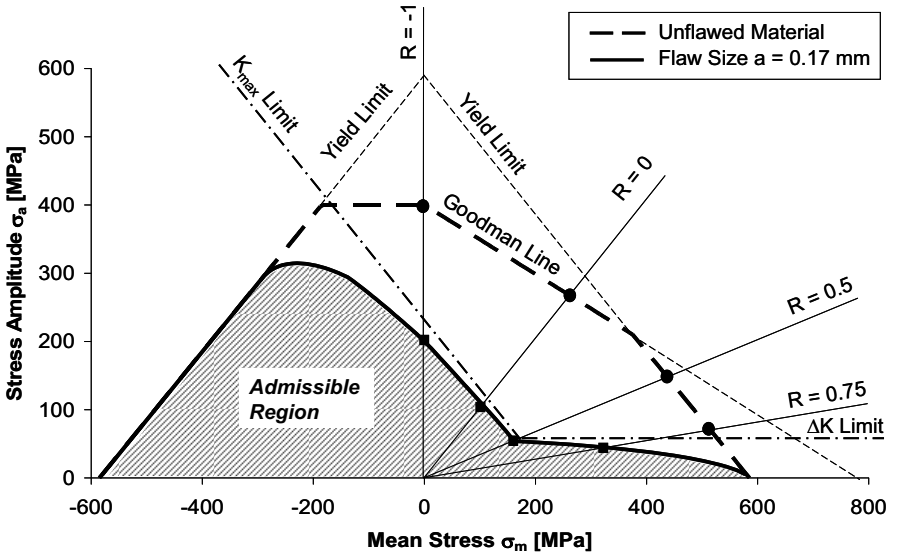

Fig. 2: Flaw size dependent Haigh diagram for S35

Gradient and Size Influence – Fatigue Notch Factors

Stress concentrations. If the material behaves according to linear elasticity, a stress concentration (such as a notch or flaw) is characterized by its elastic stress concentration factor K_t, which relates the range of the peak stress $\Delta\sigma_{max}$ to the far-field stress range $\Delta\sigma_\infty$ via

$$\Delta\sigma_{max} = K_t \Delta\sigma_\infty . \tag{5}$$

The fatigue ratio n [4] is defined by the ratio of the actual stress at the notch root at the fatigue limit, $K_t\Delta\sigma_\infty$, vs. the endurance limit of smooth specimens, $\Delta\sigma_{lim,0}$

$$n = \frac{K_t \Delta\sigma_\infty}{\Delta\sigma_{lim,0}}, \tag{6}$$

and the fatigue notch factor is defined by

$$K_f = \frac{K_t}{n} = \frac{\Delta\sigma_{lim,0}}{\Delta\sigma_\infty} . \tag{7}$$

Gradient Approaches. Experience shows that the fatigue ratio n increases with the stress concentration factor K_t, but decreases with the specimen size. The normalized stress gradient χ at hot spot ($x = 0$) accounts for both influences:

$$\chi = \mathrm{abs}\left(\frac{1}{\sigma|_{x=0}} \left(\frac{\partial\sigma}{\partial x} \right)_{x=0} \right) . \tag{8}$$

Most gradient approaches [4-6] make use of a modified power law,

$$n = 1 + \gamma \chi^{\beta} \ , \tag{9}$$

with γ = 0.45 and β = 0.3 for steel following Hueck (cf. [4]); other choices of the constants are possible depending upon the design standard used, with β typically ranging from 0.3 to 1 [4-6]. As the parameters for these correlations were calibrated from large databases compiled from analyses of typical engineering components, their range of validity does not extend beyond a stress gradient of 10 mm^{-1}.

Neuber-Novozhilov Averaging Approach. In fact, gradient concepts as presented above are conceptually quite close to averaging approaches. As an example, Neuber [7] postulates that the effective damaging stress $\overline{\sigma}$ in the notch root is computed by averaging over a characteristical microstructural length ρ^*,

$$\Delta\overline{\sigma} = \frac{1}{\rho^*} \int_0^{\rho^*} \Delta\sigma_y(x)\,\mathrm{d}x \, . \tag{10}$$

Inserting the Creager-Paris [8] solution for the stress distribution along the bisector of a notch, this gives [9]

$$\Delta\overline{\sigma} = 2\Delta\sigma_0 \sqrt{\frac{t}{\rho + 2\rho^*}} \, , \tag{11}$$

giving a fatigue notch factor of

$$K_f = \frac{\Delta\overline{\sigma}}{\Delta\sigma_0} = 2\sqrt{\frac{t}{\rho + 2\rho^*}} \tag{12}$$

and a fatigue ratio of

$$n = \frac{K_t}{K_f} = \sqrt{\frac{\rho + 2\rho^*}{\rho}} = \sqrt{1 + \chi\,\rho^*} \, . \tag{13}$$

Microcrack Averaging Approach. While Neuber [7] assumes that damage is induced over a certain material volume (or length), other authors assume pre-existing intrinsic flaws of a certain, material-specific size l_0, cf. [1]. Taking a crack-like flaw of size l_0 directly at the notch root, its SIF range follows from the Creager-Paris [8] stress distribution in the unflawed component by means of a Green's function approach [9],

$$\Delta K_I = \frac{4\Delta\sigma_\infty Y\sqrt{t}}{\sqrt{\pi\, l_0}} \int_0^{l_0} \frac{\rho + x}{(\rho + 2x)^{3/2}} \frac{1}{\sqrt{1 - (x/a)^2}}\, dx \, . \tag{14}$$

An equivalent constant stress $\Delta\overline{\sigma}$ acting along the crack flanks shall be defined such that it causes the same stress intensity as the actual stress field, i.e.,

$$\Delta K_{\mathrm{I}} = \Delta\bar{\sigma} Y \sqrt{\pi l_0} \,. \tag{15}$$

By equivalencing Eqns (14) and (15), the equivalent stress follows as

$$\Delta\bar{\sigma} = \frac{4}{\pi l_0} \Delta\sigma_\infty \sqrt{t} \int_0^{l_0} \frac{\rho + x}{(\rho + 2x)^{3/2} \sqrt{1 - (x/a)^2}} \mathrm{d}x \,, \tag{16}$$

giving a fatigue notch factor of

$$K_{\mathrm{f}} = \frac{\Delta\bar{\sigma}}{\Delta\sigma_\infty} = \frac{4}{\pi l_0} \sqrt{t} \int_0^{l_0} \frac{\rho + x}{(\rho + 2x)^{3/2} \sqrt{1 - (x/a)^2}} \mathrm{d}x \tag{17}$$

and a fatigue ratio of

$$n = \frac{K_{\mathrm{t}}}{K_{\mathrm{f}}} = \frac{\pi l_0}{2\sqrt{\rho} \int_0^{l_0} \frac{\rho + x}{(\rho + 2x)^{3/2} \sqrt{1 - (x/a)^2}} \mathrm{d}x} \,. \tag{18}$$

Crack Arrest Approach. Instead of defining an equivalent stress, the SIF range at the crack tip may directly be compared to the crack propagation threshold SIF range. Above a certain stress gradient, cracks up to a certain size may be arrested due to increasing crack closure effects while the stress at the crack tip is decreasing; for details, cf. [9].

Comparison of the approaches presented. Fig. 3 compares the predictions from the different models in terms of the dependence of the fatigue ratio $n = K_{\mathrm{t}} / K_{\mathrm{f}}$ on the normalized stress gradient $\chi = 2 / \rho$. For small stress gradients, the gradient approaches on one hand and the averaging approaches on the other hand lie very close together. As an explanation for the almost identical results of the averaging approaches, note the parallels between the resulting expressions for the fatigue ratio from microcrack averaging, Eq. (16), and from Neuber's averaging approach, Eq. (10): both are completely determined by the notch root radius ρ and the microstructural length parameter (l_0 and ρ^*, respectively). This is not surprising as, mathematically speaking, the Green's function is just a weighted average of the stresses acting perpendicular to the crack flanks.

As mentioned above, the crack arrest concept is valid only above a certain stress gradient. This value of the stress gradient is quite close to the upper end of the range of validity of the gradient models from DIN standard [6] and FKM guideline [5].

So, one could view the gradient and crack arrest concepts as mutually complementary approaches – the former for blunt stress concentrators (small n), the latter for acute, crack-like stress concentrators (large n). On the other hand, one observes that the extrapolation of the gradient predictions into the crack-like regime gives results identical to those from the crack arrest consideration so that, *formally, any stress concentration – including cracks – may be assessed by means of a gradient concept.*

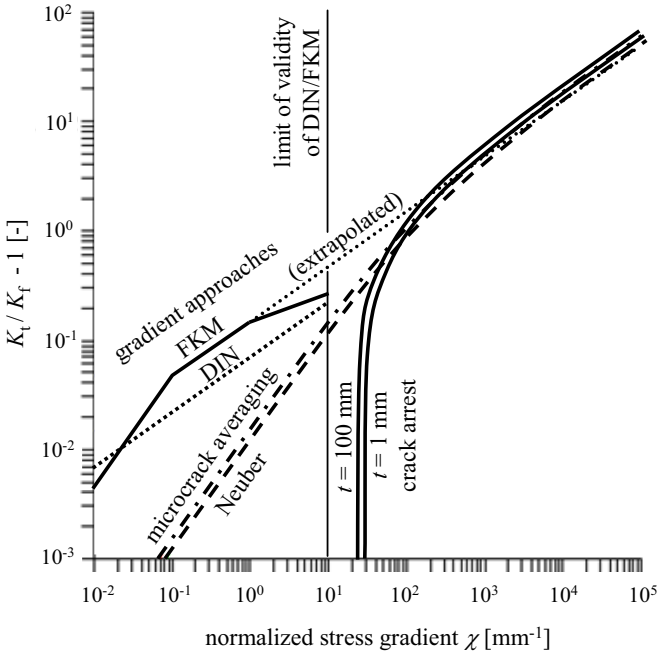

Fig. 3. Comparison of different concepts for fatigue notch factors (material: 0.6C steel).

Highly Stressed Volume Approaches. An alternative approach using the concept of highly stressed material volume was first proposed by Kuguel [10] and subsequently used and discussed by Sonsino [11], Lin and Lee [12], and Toplack *et al.* [13]. By *highly stressed volume* V_Ξ we denote that volume of material that is subjected to a stress higher than Ξ times the maximum stress encountered in the component or specimen under investigation. Typically, the 90% or 95% volume $V_{90\%}$ or $V_{95\%}$ is used. In his original paper, Kuguel [10] discusses a statistical correlation of fatigue data and observes a power-law dependence of the fatigue strength of specimens $\sigma_{\mathrm{lim},\chi}$ on the highly stressed volume V_Ξ so that, for any two specimens with indices 1 and 2, the following relation holds:

$$\frac{\sigma_{\mathrm{lim},\chi 1}}{\sigma_{\mathrm{lim},\chi 2}} = \left(\frac{V_{\Xi 1}}{V_{\Xi 2}} \right)^{\alpha_{\Xi \mathrm{V}}} . \tag{19}$$

Sonsino [11] reports the existence of a threshold volume in the range of $V_{k\infty} \approx 30\ldots60$ mm^3 beyond which no further decrease of the fatigue strength is observed (Fig. 4).

If one compares geometrically scaled specimens i of diameter 2 r_i in bending, the stress gradient $\chi_i = 1/r_i$ changes due to the scaling. The classical gradient and averaging concepts are therefore able to predict a size effect for smooth specimens in bending. One obtains

$$\frac{\sigma_{\lim 2}}{\sigma_{\lim 1}} = \frac{n_2}{n_1} = \frac{1+\gamma\chi_2^{\beta}}{1+\gamma\chi_1^{\beta}} = \frac{1+\gamma/r_2^{\beta}}{1+\gamma/r_1^{\beta}}, \tag{20}$$

$$\frac{\sigma_{\lim 2}}{\sigma_{\lim 1}} = \sqrt{\frac{1+\rho^*/r_2}{1+\rho^*/r_1}} \tag{21}$$

for the gradient concept, Eq. (9), and Neuber's averaging concept, Eq. (13), respectively.

Fig. 5 shows the predictions from the different concepts in comparison; the model parameters are chosen representative of a typical QT steel. As far as the volumetric concepts are concerned, the prediction using $\alpha_{\Xi V}$ = -0.034 as originally proposed by Kuguel is much closer to the other results in the area of interest although a choice of $\alpha_{\Xi V}$ = -0.1 gives the same asymptotic behavior as Hueck's method.

Note that, for any of the gradient or averaging concepts, the fatigue strength approaches a saturation value with increasing volume, as observed also experimentally [11]. In order to include the asymptote into the volumetric concept, the following empirical equations are proposed instead of Eq. (19):

$$\sigma_{\lim,\chi} = \sigma_{\lim\infty}\left[1+\left(\frac{V_{k\infty}}{V_{\Xi}}\right)^{-\alpha_{\Xi V}}\right], \tag{22a}$$

$$\sigma_{\lim,\chi} = \sigma_{\lim\infty}\left(1+\frac{V_{k\infty}}{V_{\Xi}}\right)^{-\alpha_{\Xi V}}, \tag{22b}$$

with the characteristical volume $V_{k\infty}$ corresponding to the volume where the saturation value of the fatigue strength for high volumes, $\sigma_{\lim\infty}$, is approached. For low highly stressed volumes $V_{\Xi} << V_{k\infty}$, the asymptotic behavior of the original Kuguel/Sonsino formula, Eq. (19), is recovered. As the *ratio* of the highly stressed volumes equals the ratio of the specimen volumes for specimens of different sizes subjected to the same loading, it is admissible to rewrite Eqns (22a,b) with the volume for the specimen dimensions near the knee point,

$$V_{k\infty} = \pi r_{k\infty}^2 l_{\infty}, \tag{23}$$

resulting in a scaling of the fatigue strength for bending specimens according to

$$\frac{\sigma_{\lim 2}}{\sigma_{\lim 1}} = \frac{1+(V_{k\infty}/V_2)^{-\alpha_{\Xi V}}}{1+(V_{k\infty}/V_1)^{-\alpha_{\Xi V}}} = \frac{1+(r_{k\infty}/r_2)^{-3\alpha_{\Xi V}}}{1+(r_{k\infty}/r_1)^{-3\alpha_{\Xi V}}}, \tag{24a}$$

$$\frac{\sigma_{\lim 2}}{\sigma_{\lim 1}} = \left(\frac{1+V_{k\infty}/V_2}{1+V_{k\infty}/V_1}\right)^{-\alpha_{\Xi V}} = \left(\frac{1+(r_{k\infty}/r_2)^3}{1+(r_{k\infty}/r_1)^3}\right)^{-\alpha_{\Xi V}}, \tag{24b}$$

which corresponds to Hueck's and Neuber's formulae, respectively.

Comparing Eqns (9) and (24a), the modified volumetric model can be made to coincide with the gradient concept if its parameters are chosen such that

$$\alpha_{\Xi V} = -\beta/3, \tag{25}$$

$$r_{k\infty} = \gamma^{1/\beta}. \tag{26}$$

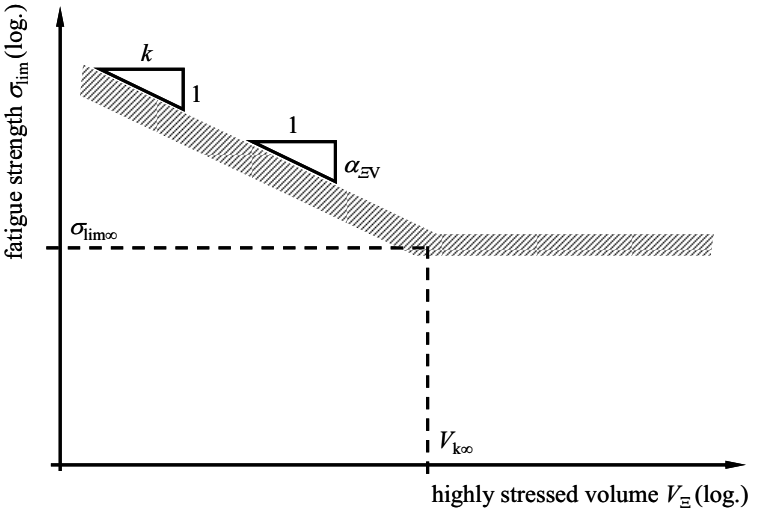

Fig. 4: Size effect.

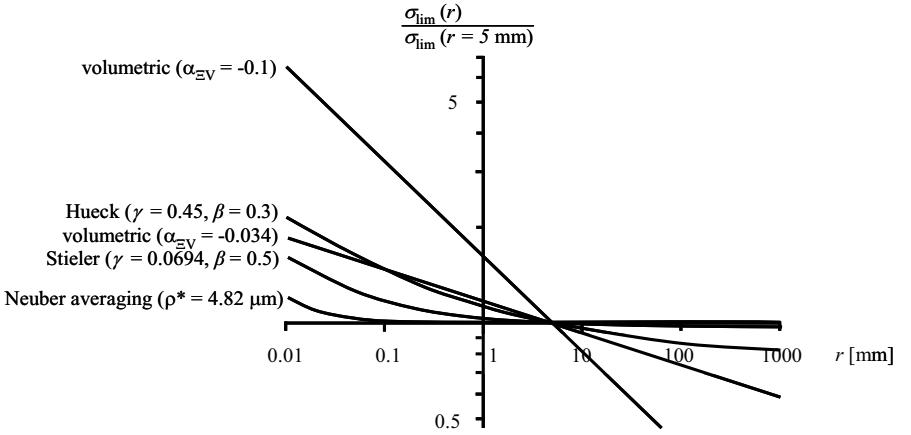

Fig. 5: Comparison of concepts for accounting for the size effect.

Summary and Conclusion

The present contribution has focused on two classical tools used in mechanical engineering for dimensioning of components: the Haigh diagram for assessing the mean stress influence, and fatigue notch factors for assessing the influence of stress concentrations.

A modified Haigh diagram has been proposed for components containing flaws that are small with respect to the macroscopic stress field.

For the assessment of macroscopic stress concentration, several concepts for computing fatigue notch factors have been re-assessed. It has turned out that gradient and modified volumetric approaches are able to capture also the behaviour of small flaws (microcracks) situated near the "hot spot" of a stress concentrator.

Combining these approaches, a fatigue strength assessment of components containing macroscopic stress concentrations together with possible flaws at the meso-/microscale is possible within the classical mechanical engineering framework of Haigh diagrams and fatigue notch factors.

References

[1] M.H. El Haddad, T.H. Topper, T.H. and K.N. Smith: Prediction of non propagating cracks. *Engng Fract. Mech.* Vol. 11 (1979) pp. 573-584

[2] H-P Gänser, A Leitgeb, K Glinsner, W Eichlseder: *Proc. Inst. Mech. Engrs Part C, J. Mech. Engng Sci. Vol.* 221 (2007) pp. 619-623

[3] Forschungskuratorium Maschinenbau (FKM): *Bruchmechanischer Festigkeitsnachweis für Maschinenbauteile (Fracture Mechanics Proof of Strength for Engineering Components*). 3rd Ed., VDMA Verlag, Frankfurt (2006)

[4] D. Radaj: *Ermüdungsfestigkeit (Fatigue strength,* in German*)*, 2nd Ed. (Springer, Berlin – Heidelberg – New York 2003)

[5] Forschungskuratorium Maschinenbau (FKM): *Rechnerischer Festigkeitsnachweis für Maschinenbauteile (Analytical Strength Assessment*). 5th Ed. (VDMA Verlag, Frankfurt 2003)

[6] DIN 743: *Tragfähigkeitsberechnung von Wellen und Achsen (Shafts and axles, calculation of load capacity)*. (Beuth Verlag, Berlin 2000)

[7] H. Neuber: *Konstruktion* 20 (1968) pp. 245-251

[8] M. Creager and P.C. Paris: Int. J. Fract. Vol. 3 (1967) pp. 247-252

[9] H.-P. Gänser, A. Leitgeb and W. Eichlseder: Synthesis of Fracture Mechanics and Stress Based Methods for Dimensioning against the Endurance Limit. In: *Proc. ICF 2007* (Moscow 2007)

[10] R. Kuguel: Proc. ASTM Vol. 61 (1961) pp. 732-748

[11] C.M. Sonsino and G. Fischer: *Mat.-wiss. u. Werkstofftech.* Vol. 36 (2005) pp. 632-641

[12] C.J. Lin and C.K. Lee: *Int. J. Fatigue* Vol. 20 (1998) pp. 301-307

[13] G. Toplack, W. Eichlseder, I. Gódor and H. Leitner: Influence of Size and Type of Loading on S/N Curve. In: *Proc. Cumulative Fatigue Damage* (Sevilla 2003)